

Article

Numerical Simulation of High-Energy, Ytterbium-Doped Amplifier Tunability

Celso P. João ^{1,*}, João Wemans ² and Gonçalo Figueira ¹

¹ Laser and Plasma Group (GoLP)/Institute for Plasmas and Nuclear Fusion- Associate Laboratory, Instituto Superior Técnico, Lisbon 1049-001, Portugal; E-Mail: goncalo.figueira@ist.utl.pt

² WS Energia, Taguspark, Porto Salvo 2740-257, Portugal; E-Mail: wemans@ws-energia.com

* Author to whom correspondence should be addressed; E-Mail: celsopaivajoao@ist.utl.pt; Tel.: +351-218-419-275; Fax: +351-218-464-455.

Received: 17 December 2012; in revised form: 30 January 2013 / Accepted: 27 February 2013 /

Published: 13 March 2013

Abstract: The study of wavelength tunability for the gain media Yb:CaF₂ and Yb:YAG in a regenerative amplifier configuration, was performed by using a simulation code previously benchmarked with real data. The results demonstrate that both materials have potential for amplifying pulses up to the milijoule level for wavelengths around 1048–1049 nm. In light of this, we propose and evaluate their performance as gain media in the pre-amplifier of a hybrid chain operating at 1053 nm.

Keywords: laser amplifiers; simulation; ytterbium lasers; diode-pumped lasers; neodymium lasers

1. Introduction

In recent years, the sustained development of high power diode lasers and their application as pump devices in high peak and average power lasers have contributed to a growing research in different ytterbium-doped materials. In fact, the combination of these gain media and diode pumping has proved to be an extremely valuable option for development of dedicated systems for pumping high-energy, high repetition rate, ultrashort duration optical parametric amplifiers [1] and it is also a promising choice for the development of Yb-based chirped pulse amplification (CPA) systems on their own, aimed at reaching multi-Joule pulses in the sub-picosecond regime [2].

The interest in Yb-doped media is justified by their unique spectroscopic properties bringing more advantages for diode pumping than other traditional gain media [3]. They exhibit a broadband absorption cross-section and high fluorescence lifetime at milisecond time scales, low quantum defect and a simple electronic structure that avoids some parasitic effects. All these properties allow them to be pumped very efficiently at very high repetition rates by low-brightness semiconductor lasers with emission peaks in range 920 to 980 nm. Additionally, these media exhibit a large gain bandwidth in the spectral range between 1020 and 1070 nm capable of supporting ultrashort pulses lasting tens of femtoseconds, as was recently demonstrated by using $\text{Yb}^{3+}:\text{CaGdAlO}_4$ (Yb:CALGO) to generate 40 fs pulses [4].

A large number of Yb-doped hosts have been investigated, characterized by slight differences in their spectroscopic parameters depending on the host family. This great variety leads to a considerable sensitivity to the laser parameters, requiring a careful and reliable modeling in order to evaluate the performance of a given system in terms of e.g., wavelength tunability and bandwidth evolution over the course of regenerative or multipass amplification. In particular, in a regenerative amplifier the modeling is significantly more useful since the net gain of the amplification stage is usually 10^4 to 10^6 and the usually low single-pass-gain results in high number of round-trips [5]. For this reason, we have previously developed a simulation code that was benchmarked with real experimental data, in order to test and evaluate the laser performances of different Yb-doped gain media [6].

On the other hand, it is well known that flashlamp-pumped Nd:glass laser systems operating at 1053 nm are still a well-established technology for reaching pulsed energies above the kJ range with a lower cost per Joule. Petawatt level, Nd:glass-based CPA systems have been demonstrated, using high-performance front-ends based e.g., in regenerative amplification in Ti:sapphire or broadband parametric amplification. Fully ytterbium-based amplification systems are limited to 10 J [7] but they already represent a very competitive option up to Joule level [8,9], making them an interesting alternative for the pre-amplifier stages of a high energy/high power Nd:glass laser, provided they can perform efficiently at the required wavelength. Recent progress towards this hybrid amplification concept has consisted in the demonstration of a Q-switched cavity based in Yb:CaF₂ extending from 1028 to 1065 nm [10], and the development of high-efficiency Yb:YAG laser oscillators operating at 1048–1050 nm [11,12], although with pulse energies limited to a few tens of nanojoules.

In this work, we evaluate numerically the energy and spectral performance for the gain media Yb:YAG and Yb:CaF₂ for different pump powers when used in a diode-pumped regenerative amplifier. The goal is to explore the tunability of these materials around 1053 nm and evaluate their application in the pre-amplifier stages of an Nd:glass-based power amplifier chain, up to the Joule level. The main difference with respect to our previous study [6] is that here we show that Yb:YAG can effectively be used as a suitable, high-energy gain material around 1049 nm, whereas, before the tunability, it was limited around its strong gain peak at ~1030 nm. We demonstrate that a careful choice of pumping parameters allows tuning an Yb:YAG amplifier between one wavelength and another. The motivation for this work arises from the fact that the electrical to optical efficiency of diode pumping can be a few orders of magnitude greater than that of flashlamp pumping, which becomes of central importance e.g., for large scale, multi-beam Nd:glass lasers.

2. Numerical Simulation of Ytterbium-Based Amplification

2.1. Introduction

As described in our previous work, we have developed a one-dimensional numerical code for modeling energy, gain and spectral performance of an ytterbium-based regenerative amplifier, to which we have added routine for the spectral response of a generic Nd:glass amplifier following the first stage. The model for ytterbium-based amplification can be applied to different host materials and consists of two routines: the first one simulates the pump process and calculates the pump absorption and population inversion, and the second one simulates the overall amplification process calculating the pulse energy and spectrum after each pass through the gain medium. Both routines are ruled by the following discrete rate equations:

$$\frac{dN_{ex}(z,t)}{dt} = -\frac{N_{ex}(z,t)}{\tau_f} + \left[\sigma_a(\lambda)N_{grd}(z,t) - \sigma_e(\lambda)N_{ex}(z,t) \right] \frac{\lambda}{hc} I(z,t) \quad (1)$$

$$\frac{dI(z,t)}{dz} = \left[\sigma_e(\lambda)N_{ex}(z,t) - \sigma_a(\lambda)N_{grd}(z,t) \right] I(z,t) \quad (2)$$

where N_{ex} is the excited state population, N_{grd} is the ground state population, (z,t) are the longitudinal position and time inside the gain medium, I is the wavelength-dependent pulse intensity, λ is the wavelength, σ_a and σ_e are respectively the absorption and emission cross-sections, τ_f is the fluorescence lifetime, h is Planck's constant and c is the speed of light in vacuum.

Ytterbium-doped laser media are described by a quasi-three-level model where the relevant laser transitions take place between the sub-levels of two manifolds, the ground-state $^2F_{7/2}$ and the excited state $^2F_{5/2}$. At room temperature, the sub-levels of the ground-state manifold are thermally populated due to the proximity between them, and in consequence reabsorption losses can be generated at the laser wavelength. This property has the drawback of making ytterbium lasers inefficient for very low pump intensities, but it can also be used beneficially in order to explore different sub-level transitions. This effectively means that one is able to tune the laser amplifier for different wavelengths by changing the pump power.

Two good candidates for efficient laser amplification near 1053 nm are Yb:CaF₂ and Yb:YAG, in the first case because of the relatively broad tunability [10], and in the second because of the presence of a peak in the emission cross-section near this wavelength. We have used spectroscopic data for both materials (Figure 1) [13] and evaluated their amplification performance under different pump powers.

Table 1 lists the parameters that were used for the two materials. Where realistic input parameters for the pump source and the laser media were required, we have assumed typical values without loss of generality. The chosen pump pulse length matches the fluorescence lifetime of each gain media, *i.e.*, 2.4 ms for Yb:CaF₂ and 1 ms for Yb:YAG. It is assumed that the gain medium is longitudinally pumped in a two-pass configuration, in order to reach a high population inversion in Yb:CaF₂. The focused pump spot FWHM diameter is 700 μ m. For Yb:CaF₂ we have considered 5 at% doping level and a length of 3.8 mm, while for Yb:YAG the doping level is 3 at% and the length is 8 mm. Furthermore no considerations about the damage threshold of the items in the cavity were taken into account.

Figure 1. Absorption (solid lines) and emission (dashed lines) for Yb:CaF₂ (green) and Yb:YAG (blue). Adapted from Ref. [13].

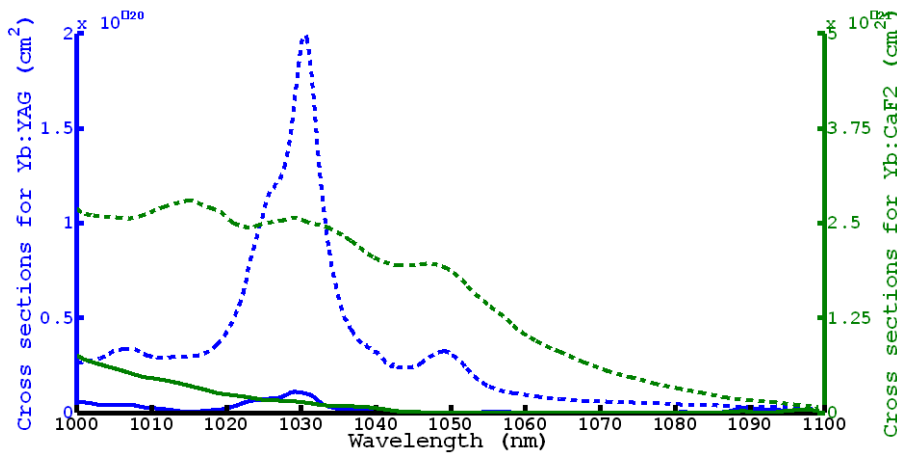


Table 1. Parameters used in the numerical simulations.

Parameter	Yb:CaF ₂	Yb:YAG
Pump pulse		
Power (W)	46–66	20–30
Duration (ms)	2.4	1
Beam diameter (mm)	0.7	0.7
Wavelength (nm)	938	938
Seed pulse		
Energy (pJ)	100	100
Duration (ns)	1	1
Beam diameter (mm)	0.7	0.7
FWHM Bandwidth (nm)	12	12
Gain medium		
Length (mm)	3.8	8
Yb ³⁺ concentration (at %)	5	3

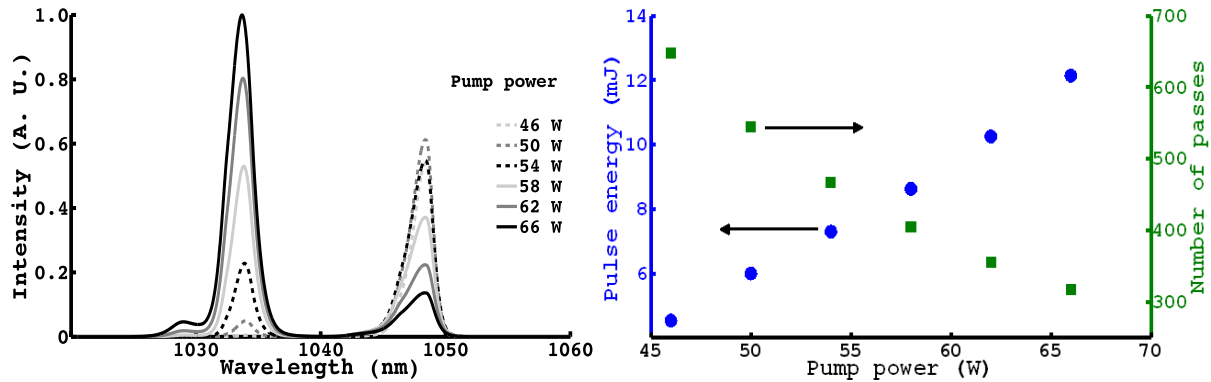
2.2. Regenerative Amplifier: Free-Running Cavity

In this section we will make a preliminary evaluation of the wavelength tunability for both media considering a free-running cavity, *i.e.*, where amplified stimulated emission grows from noise rather than from a seed pulse. The amplified pulse is then extracted at the peak energy. The initial pulse traveling in the cavity has a rectangular spectral profile between 1020 and 1060 nm and an energy of 10⁻⁶ nJ, corresponding to ~1 photon for each wavelength slice used in the calculation. The pulse duration is 10 ns, which is similar to that obtained by cavity-dumping. We assume that there is no spectral filtering in the cavity (apart from the gain-induced modulation), so losses are equal for all wavelengths.

Figures 2 (Yb:CaF₂) and 3 (Yb:YAG) show the results in terms of output spectrum (left) and energy (right) performance *vs.* pump power. For two discrete ranges of pump powers, 46–66 W for Yb:CaF₂

and 20–30 W for Yb:YAG, we have determined the maximum energy extractable and the number of roundtrips needed to achieve it.

Figure 2. Simulation of free-running cavity based in Yb:CaF₂. Left: Output intensity vs. wavelength for a range of pump power; right: output energy and required number of passes vs. pump power.



A common trend to both media is immediately apparent: for lower pump powers, there is a significant fraction of the amplified spectrum centered around 1048–1050 nm, corresponding to the case of a lower population inversion. As the pump power increases, gain shifting brings the spectral peak down to ~1030–1035 nm, resulting from the higher population inversion. The spectral distribution is however different for each case. For Yb:CaF₂ at the lowest pump power we observe a broad peak centered at 1048 nm. As the pump power is raised, the output energy is transferred to a second peak which forms around 1034 nm. At higher powers (54–58 W) it is possible to obtain a balance in the energy distribution between the two peaks. By increasing the pump power even further the longer wavelength peak will eventually vanish and the second one increases and slightly shifts towards lower wavelengths. This behavior confirms experimental results reported for different pump conditions by S. Ricaud *et al.* [14].

For Yb:YAG, a similar evolution is numerically witnessed, although the transition is more abrupt and the parameters are much more restrictive. The pump power required to overcome the lasing threshold (~20 W) is very close to that when the output spectrum is shifted to 1032 nm (~26 W), leaving a narrow range of pump powers and cavity loss combinations that allow amplification at 1049 nm. As a consequence of this, more than a thousand passes become necessary to reach high energies at this wavelength, as can be seen in Figure 3 (right). In contrast, an Yb:CaF₂ amplifier operating at a similar wavelength would only require less than half the passes. This should be taken in consideration for the practical development of mJ-level amplifiers at 1050 nm based in Yb:YAG.

The behavior described above can be understood recurring to a model for the population inversion at the two different wavelength regions. Taking the case of Yb:YAG, Figure 4 shows its energy level scheme, that can be considered a quasi-4 level. Both the ground level and the upper level are located within manifolds, separated by approximately 10,000 cm⁻¹. The absorption line at 941 nm is represented, as well as two transitions between (i) sublevels f_4 (10327 cm⁻¹) and f_3 (785 cm⁻¹), corresponding to the lasing wavelength 1048 nm, and (ii) sublevels f_4 and f_2 (612 cm⁻¹), corresponding

to the wavelength 1029 nm. The figure also indicates the relative thermal occupancies for each manifold at a temperature of 300 K, assuming a Boltzmann distribution of the energy levels.

Figure 3. Simulation of free-running cavity based in Yb:YAG. **Left:** Output intensity vs. wavelength for a range of pump power; **Right:** output energy and required number of passes vs. pump power.

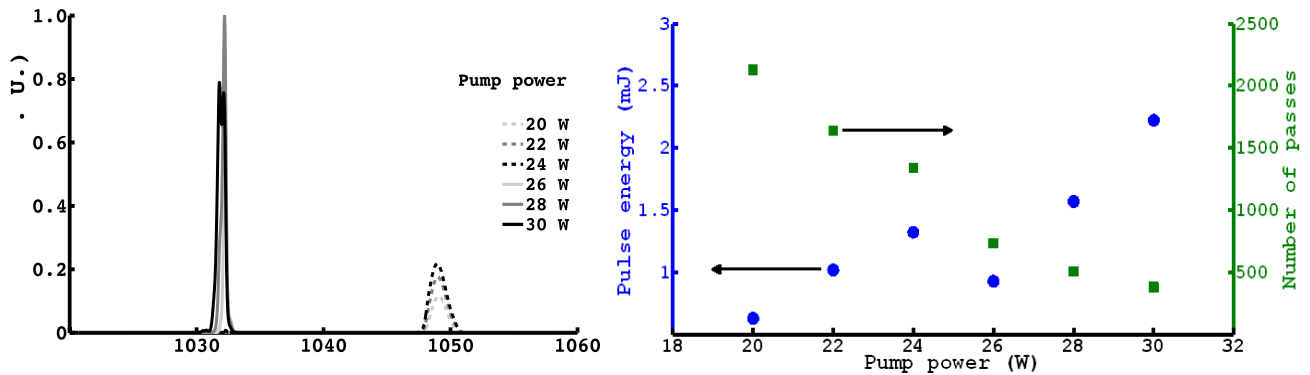
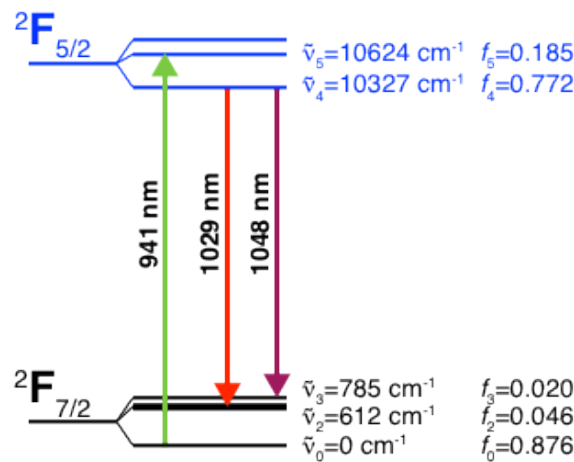


Figure 4. Energy level scheme and laser transitions in Yb:YAG.



From the rate equations for the pump process, one can arrive at the following expression for the population difference, relating the population densities of the upper manifold n_U and lower manifold n_L , and the thermal occupancies of the relevant levels [15]:

$$\Delta n_{4m} = f_4 n_U - f_m n_L, \quad m = (2, 3) \tag{3}$$

The full expressions for the population densities account for the absorption and stimulated emission cross-sections σ_a and σ_e , the fluorescence lifetime τ_f and the pump rate W , and may be found in the cited reference. The pump rate is defined as

$$W = \frac{P_{\text{pump}} \eta \lambda_p}{h c \pi r^2 l n_d} \tag{4}$$

where P_{pump} is the pump power, η is the excitation efficiency, λ_p is the wavelength, r is the radius of the excited region and l is the length of the Yb:YAG crystal. By replacing the values used in our simulation and making $\Delta n_{4m} = 0$, we find the pump power thresholds at which the population difference becomes positive, and amplification is possible (not taking cavity roundtrip losses into

account). We arrive at the following values: $P_{thr}(1048 \text{ nm}) = 11.2 \text{ W}$, $P_{thr}(1029 \text{ nm}) = 25.2 \text{ W}$, closely matching the results of the simulation. This shows that there is a range of powers where amplification at the main peak wavelength is effectively suppressed due to the higher absorption, and operation around 1048 nm is possible. As soon as the upper pump threshold is reached, the larger gain cross-section at 1029 nm becomes prevalent.

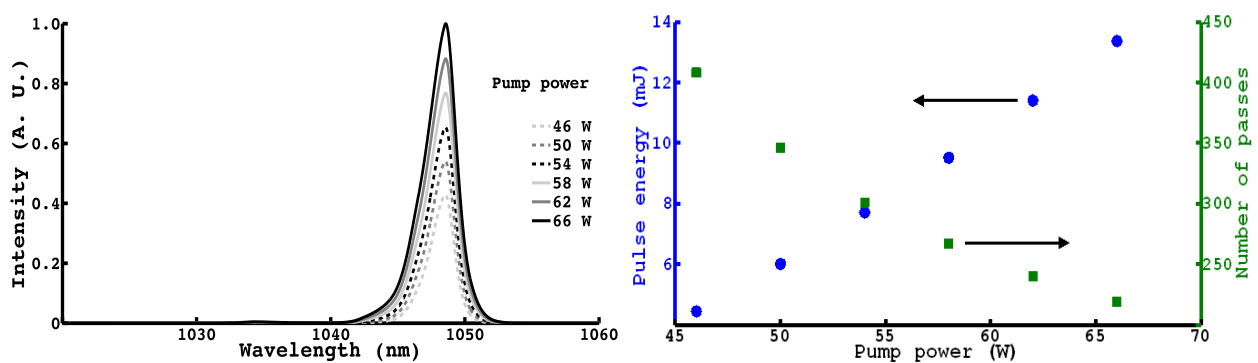
2.3. Regenerative Amplifier: Seeded Cavity

We now consider the evolution of an input pulse inside a regenerative amplifier *i.e.*, a seeded cavity, for different pump powers. The input is chosen to be a Gaussian pulse centered at 1053 nm with a FWHM bandwidth of 12 nm, well inside the gain bandwidth of both media. Although the initial spectral response of the system is identical, one can expect that the evolution will be now be determined by these significantly different initial conditions. All other parameters are the same as in the previous section (Table 1). Again, the output parameters are taken at the maximum pulse energy.

It is important to notice that since we are not considering any spectral filtering or hard spectral clip on the input pulse, its spectrum spreads infinitely, leaving a residual finite energy at lower wavelengths. For instance, for the parameters above the intensity at 1034 nm and 1032 nm will be respectively $\sim 10^{-3}$ and $\sim 2 \times 10^{-4}$ times that at 1053 nm. Such values can be considered as noise inside the cavity, and from the results of the previous section we can expect their role in the amplification process to become more significant as the pump power increases.

Figure 5 (left) shows the results for Yb:CaF₂ for pump powers between 46–66 W. Contrary to the previous section we now observe that the output spectrum remains centered around 1049 nm for the entire pump power range. There is also a slight broadening (2.1 to 2.7 nm) towards the lower wavelengths due to the reduced reabsorption for higher population inversions. Besides, seeding the cavity allows reaching a higher output energy in a lower number of roundtrips for the same pump conditions due to the lower percentage of global losses.

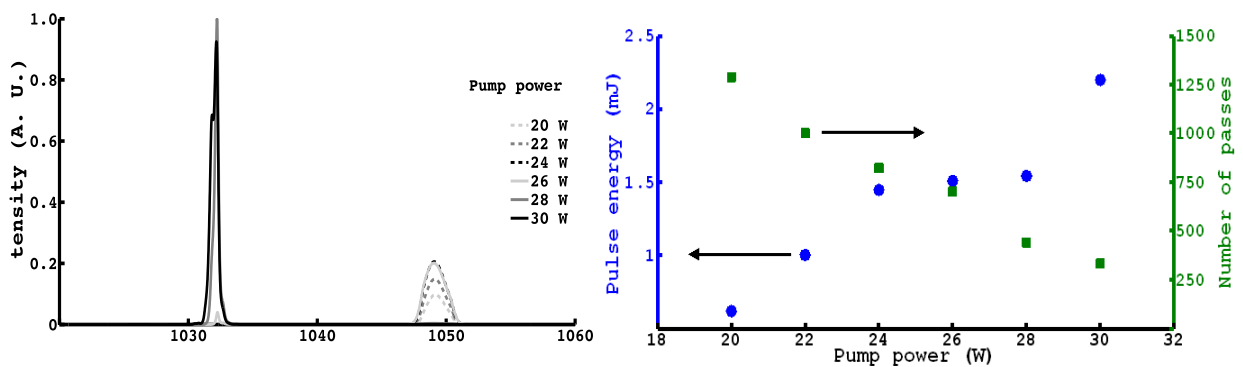
Figure 5. Simulation of regenerative amplification based in Yb:CaF₂ in injection mode. **Left:** Output intensity vs. wavelength for a range of pump power; **Right:** output energy and required number of passes vs. pump power.



The results for Yb:YAG are presented in Figure 6. The major difference is that there is still an abrupt transition around 26–28 W where the output central wavelength changes from 1049 to 1032 nm, in spite of the injected signal. The reason for this difference between the two materials lies in their

emission and absorption cross-sections. Yb:CaF₂ exhibits smoothly-varying curves between 1020 and 1080 nm (Figure 1), such that small changes in the population inversion do not cause an abrupt transition between the lasing wavelengths. On the other hand, the very strong emission peak of Yb:YAG around 1030 nm (~8 × greater than that at 1050 nm) becomes dominant once the population inversion is favorable. Although it is possible to achieve mJ-level output energies at 1049 nm, more than 800 passes are required. One option could be the use of additional spectral filtering in the cavity by means of e.g., polarizers, etalons or dichroic mirrors, thereby allowing stronger pumping.

Figure 6. Simulation of regenerative amplification based in Yb:YAG in injection mode. **Left:** Output intensity vs. wavelength for a range of pump power; **Right:** output energy and required number of passes vs. pump power.



2.4. Ytterbium-Neodymium Hybrid Amplification Chain

The last results show that both materials can be considered promising candidates for millijoule-level regenerative amplification at ~1049 nm. Since the gap between this wavelength and the emission peak wavelength of Nd:glass (phosphate) at 1053 nm is very small, one can envisage their use in the pre-amplifier stages in a hybrid laser chain.

For evaluating this possibility, we used a simple routine based on the spectral response of an Nd:glass amplifier that is fed with the output data from the previous ytterbium-based amplification routine, such as energy and spectrum. The amplifier is modeled as a single-pass in an Nd:glass slab working far from saturation, described by the following unsaturated gain equation:

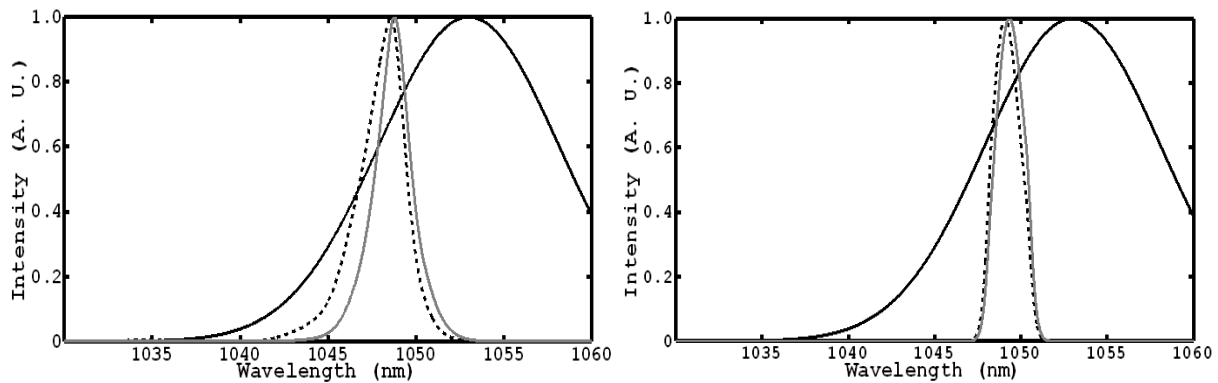
$$I_{out}(\lambda) = I_{in}(\lambda)e^{\sigma_e(\lambda)NL} \quad (5)$$

Here I_{in} and I_{out} are the spectral intensities of the pulse before and after the amplification, σ_e is emission cross-section of Nd:glass, N is the inverted population density, and L is the length of the gain medium.

For this hybrid configuration we chose the same realistic input parameters than for the previous simulations. The pump pulse, seed pulse and crystal parameters are those used in the previous section with the exception of the pump powers that were chosen to be 66 W for Yb:CaF₂ and 24 W for Yb:YAG, due to the favorable percentage of inverted population for amplification near 1053 nm and to prevent the generation of undesired high energy amplified spontaneous emission (ASE) that competed with the main pulse. We assume a 23.5 cm long Nd:glass with an inverted population density of $7.5 \times 10^{18} \text{ cm}^{-3}$.

Figure 7 shows the output spectra calculated for the two hybrid chain combinations. The pre-amplified and final pulse energies for Yb:CaF₂ were 13.4 mJ (after 219 passes) and 1.43 J while for Yb:YAG we obtained 1.4 mJ (822 passes) and 230 mJ respectively. For both cases there is strong gain narrowing during the pre-amplification stage, leading to a final bandwidth of 2 nm.

Figure 7. Output spectra for a hybrid amplification chain with pre-amplifier based with Yb:CaF₂ (**left**) and Yb:YAG (**right**). The solid black line represents the initial spectrum, the black dashed line the output spectrum from the pre-amplifier and the grey line the output spectrum after the power amplifier.



These results confirm that both Yb-doped media studied here are viable alternative pre-amplifier stages for a hybrid amplification chain operating at 1053 nm. However, the number of passes for a millijoule-level Yb:YAG amplifier is typically much larger.

3. Conclusions

This work has shown that it is feasible to conceive mJ-level regenerative amplification based in Yb:CaF₂ and Yb:YAG that can be tuned between two spectral peaks (1034–1048 nm in the first case and 1032–1049 nm in the second) by changing only the pump power of the system. The simulations also show that achieving amplification at 1049 nm with Yb:YAG is harder than for Yb:CaF₂ at 1048 nm due to the more restrictive set of parameters available, namely the need to use a low pump power near to the gain threshold, and low cavity losses. This however still results in a very high number of passes, often in excess of 1000.

The favorable tunability properties of Yb:CaF₂ and Yb:YAG for wavelengths around 1050 nm make them natural candidates for pre-amplifier stages of systems based in Nd:glass power amplifiers. We have explored this possibility by simulating two hybrid amplification chains for both gain media, seeded with a 12 nm signal centered at 1053 nm. Both amplifiers allow obtaining output pulse energies above the mJ range, with a bandwidth of 2–3 nm. While this is too narrow for generating ultrashort pulses, it is acceptable in energy-oriented, sub-picosecond glass lasers. Finally the last amplification stage boosts this energy by two orders of magnitude without significantly narrowing the spectrum. In conclusion, ytterbium-based regenerative amplification may prove a suitable technological option for large-scale, multi-beam, high energy Nd:glass chains where efficiency is a major requirement.

Acknowledgments

This work was partially supported by Fundação para a Ciência e a Tecnologia (grant SFRH/BD/68865/2010), Associação Euratom-IST and LASERLAB-Europe III. The values for the cross-sections at room temperature used in our simulations were provided courtesy of J. Körner and J. Hein, Institute of Optics and Quantum Electronics, Friedrich-Schiller-University of Jena.

References

1. Klingebiel, A.; Wandt, C.; Skrobol, C.; Ahmad, I.; Trushin, S.A.; Major, Z.; Krausz, F.; Karsch, S. High energy picosecond Yb:YAG CPA system at 10 Hz repetition rate for pumping optical parametric amplifiers. *Opt. Express* **2011**, *19*, 5357–5363.
2. Hein, J.; Kaluza, M.C.; Bödefeld, R.; Siebold, M.; Podleska, S.; Sauerbrey, R. Polaris: An All Diode-Pumped Ultrahigh Peak Power Laser for High Repetition Rates. In *Laser and Nuclei, Lecture Notes in Physics*; Springer: Berlin, Germany, 2006; Volume 694, pp. 47–66.
3. Druon, F.; Balembos, F.; Georges, P. New laser crystals for the generation of ultrashort pulses. *C.R. Physique* **2007**, *8*, 153–164.
4. Agnesi, A.; Greborio, A.; Pirzio, F.; Reali, G.; Aus der Au, J.; Guandalini, A. 40-fs Yb³⁺:CaGdAlO₄ laser pumped by a single-mode 350-mW laser diode. *Opt. Express* **2012**, *20*, 10077–10082.
5. Raybaut, P.; Balembos, F.; Druon, F.; Georges, P. Numerical and experimental study of gain narrowing in ytterbium-based regenerative amplifiers. *IEEE J. Quant. Electron.* **2005**, *41*, 415–425.
6. Wemans, J.; João, C.P.; Figueira, G. Evaluation of hybrid ytterbium–neodymium laser amplification at 1053 nm. *Appl. Phys. B* **2010**, *101*, 103–108.
7. Banerjee, S.; Ertel, K.; Mason, P.D.; Phillips, P.J.; Siebold, M.; Loeser, M.; Hernandez-Gomez, C.; Collier, J.L. High-Efficiency 10 J diode pumped cryogenic gas cooled Yb:YAG multislabs amplifier. *Opt. Lett.* **2012**, *37*, 2175–2177.
8. Tümmler, J.; Jung, R.; Stiel, H.; Nickles, P.V.; Sandner, W. High-Repetition-rate chirped-pulse-amplification thin-disk laser system with joule-level pulse energy. *Opt. Lett.* **2009**, *34*, 1378–1380.
9. Siebold, M.; Loeser, M.; Schramm, U.; Koerner, J.; Wolf, M.; Hellwing, M.; Hein, J.; Ertel, K. High-Efficiency, room-temperature nanosecond Yb:YAG laser. *Opt. Express* **2009**, *17*, 19887–19893.
10. Courjaud, A.; Clet, V.; Doualan, J.L.; Camy, P.; Moncorgé, R.; Mottay, E. Yb:CaF₂ Diode-Pumped Millijoule Nanosecond Laser Tunable from 1030 to 1065 nm. In Proceedings of Conference on Lasers and Electro-Optics (CLEO), San Jose, CA, USA, 6–11 May 2012.
11. Zhou, B.; Wei, Z.; Li, D.; Teng, H.; Bourdet, G.L. Generation of 170-fs laser pulses at 1053 nm by a passively mode-locked Yb:YAG laser. *Chin. Phys. Lett.* **2009**, *26*, 054208:1–054208:3.
12. Zhou, B.; Wei, Z.; Zou, Y.; Zhang, Y.; Zhong, X.; Bourdet, G.L.; Wang, J. High-efficiency diode-pumped femtosecond Yb:YAG ceramic laser. *Opt. Lett.* **2010**, *35*, 288–290.

13. Koerner, J.; Vorholt, C.; Liebetrau, H.; Kahle, M.; Kloepfel, D.; Seifert, R.; Hein, J.; Kaluza, M.C. Measurement of temperature-dependent absorption and emission spectra of Yb:YAG, Yb:LuAG, and Yb:CaF₂ between 20 °C and 200 °C and predictions on their influence on laser performance. *J. Opt. Soc. Am. B* **2012**, *29*, 2493–2502.
14. Ricaud, S.; Druon, F.; Papadopoulos, D.N.; Camy, P.; Doualan, J.L.; Moncorgé, R.; Delaigue, M.; Zaouter, Y.; Courjaud, A.; Georges, P.; *et al.* Short-pulse and high-repetition-rate diode-pumped Yb:CaF₂ regenerative amplifier. *Opt. Lett.* **2010**, *35*, 2415–2417.
15. Ostermeyer, M.; Straesser, A. Theoretical investigations of feasibility of Yb:YAG as laser material for nanosecond pulse emission with large energies in the Joule range. *Opt. Comm.* **2007**, *274*, 422–428.

© 2013 by the authors; licensee MDPI, Basel, Switzerland. This article is an open access article distributed under the terms and conditions of the Creative Commons Attribution license (<http://creativecommons.org/licenses/by/3.0/>).